Available online at www.sciencedirect.com
SCIENCE DIRECT®
ELSEVIER
International Journal of Multiphase Flow 30 (2004) 697–710
International Journal of Multiphase Flow
www.elsevier.com/locate/ijmulflow

Single bubble growth in saturated pool boiling of binary mixtures

Han Choon Lee, Jeongbae Kim, Byung Do Oh, Moo Hwan Kim *

Department of Mechanical Engineering, Pohang University of Science and Technology, San 31, Hyoja-dong, Namgu, Pohang, Kyoungbuk 790-784, Republic of Korea

Received 28 November 2003; received in revised form 12 March 2004

Abstract

Nucleate pool boiling experiments for binary mixtures, which are consisted of R11 and R113, were performed with constant wall temperature condition. Results for binary mixtures were also compared with pure fluids. A microscale heater array and Wheatstone bridge circuits were used to maintain the constant temperature of the heating surface and to obtain heat flow rate measurements with high temporal and spatial resolutions. Bubble growth images were captured using a high-speed CCD camera synchronized with the heat flow rate measurements.

The departure time for binary mixtures was longer than that for pure fluids, and binary mixtures had a higher onset of nucleate boiling (ONB) temperature than pure fluids. In the asymptotic growth region, the bubble growth rate was proportional to a value between $t^{1/6}$ and $t^{1/4}$. The bubble growth behavior was analyzed to permit comparisons with binary mixtures and pure fluids at the same scale using dimensionless parameters. There was no discernible difference in the bubble growth behavior between binary mixtures and pure fluids for a given ONB temperature. And the departure radius and time were well predicted within a $\pm 30\%$ error.

The minimum heat transfer coefficient of binary mixtures occurred near the maximum $|y - x|$ value, and the average required heat flux during bubble growth did not depend on the mass fraction of R11 as more volatile component in binary mixtures. Finally, the results showed that for binary mixtures, a higher ONB temperature had the greatest effect on reducing the heat transfer coefficient.

Keywords: Binary mixture; Saturated pool boiling; Constant wall temperature; Single bubble growth; Heat transfer coefficient; Microscale heater array

* Corresponding author. Tel.: +82-54-279-2165; fax: +82-54-279-3199.
E-mail address: mhkim@postech.ac.kr (M.H. Kim).

0301-9322/$ - see front matter © 2004 Elsevier Ltd. All rights reserved.
doi:10.1016/j.ijmultiphaseflow.2004.05.007

1. Introduction

The boiling characteristic of binary mixtures is supposed to differ from those of pure fluids due to differences in their heat transfer rates, as the heat transfer rate of mixtures is generally lower than that of an equivalent ideal pure fluid. Most previous researchers have explained the heat transfer rate reduction as being due to the concentration boundary layer on the liquid side. However, the onset of nucleate boiling (ONB) temperature is also one of the important factors that can reduce the heat transfer rate of mixtures. In the present study, heat transfer rate deterioration was examined through single bubble growth experiments at saturated pool boiling for binary mixtures. The heat transfer coefficients for growth of single bubbles of binary mixtures at the near ONB temperatures were evaluated and compared with these of pure fluids.

Scriven (1959) investigated the theoretical bubble growth rate in the bulk of a binary mixture. Starting with the fundamental relationships of continuity, momentum, energy, and mass diffusion, he produced a bubble growth equation as a function of time. Van Stralen (1966) modified Scriven's equation for the bubble growth rate using an alternative method for considering the difference between the apparent and actual superheats. His growth equation is quite similar to Scriven's equation and can be transformed into a convenient form that contains the resistance factor $|y-x|$ in the denominator. Here, y is the mass fraction of the more volatile component on the vapor side, and x is the mass fraction of the more volatile component on the liquid side.

Based on theoretical analyses, many researchers have suggested the correlations for the heat transfer coefficient of mixtures using the reduction factor like as $|y-x|$. Stephan and Korner (1969) developed an empirical correlation for the wall superheat at a given heat flux. They concluded that the energy required to form a vapor bubble in a binary mixture is a function of the mass transfer driving force, $|y-x|$, and obtained a heat transfer correlation that was a function of the wall superheat. Calus and Leonidopoulos (1974) also used Scriven's result and suggested a heat transfer correlation for a binary mixture based on the wall superheat like

$$h = \frac{h_i}{1 + 1.53(0.88 + 0.12p)|y-x|}, \quad h_i = \frac{1}{\frac{x}{h_1} + \frac{1-x}{h_2}} \tag{1}$$

Here, h is heat transfer coefficient of binary mixture, h_1 is that of pure non-volatile component, h_2 is that of pure volatile component, and P is pressure.

Calus and Rice (1972) attempted to quantitatively relate the reduction in the heat transfer coefficient to reduction in the bubble growth rate as

$$h = \frac{h_i}{\left[1 + |y-x|\left(\frac{\alpha}{D}\right)^{0.5}\right]^{0.7}} \tag{2}$$

Here, α is thermal diffusivity of liquid and D is liquid mass diffusivity.

Other researchers have also attempted to correlate the heat transfer coefficient for a binary mixture with the resistance factor, $|y-x|$. Celata et al. (1994) reviewed heat transfer correlations for pool boiling of binary mixtures. Unal (1986) proposed a correlation based on an empirical procedure of dimensional analysis that allowed to him to obtain as Eq. (3).

$$h = \frac{h_i}{[1 + (b_2 + b_3)(1 + b_4)][1 + b_5]} \tag{3}$$

$$b_2 = (1 - x)\ln\frac{1.01 - x}{1.01 - y} + x\ln\frac{x}{y} + |y - x|^{1.5}, \quad \frac{x}{y} = 1 \text{ for } x = y = 0$$

$$b_3 = 0,\ b_4 = 152\left(\frac{p}{p_c}\right)^{3.9}, \quad b_5 = 0.92|y - x|^{0.001}\left(\frac{p}{p_c}\right)^{0.66}$$

Here, p_c is critical pressure of the volatile component.

The previous correlations given like as Eqs. (1)–(3) were proposed assuming a constant bubble frequency, bubble growth, nucleation site density, and ONB temperature. All of these factors can affect the heat flow rate and the heat transfer coefficient. In the present experiments, the heat transfer coefficient was evaluated for one period of growth for a single bubble at one nucleation site with a constant wall temperature. The heat transfer characteristics of binary mixtures were compared with those of pure fluids at the near each ONB temperatures.

Most of the previous research on single bubble growth has been performed using a constant wall heat flux created by heating a metallic block beneath the bubble. However, the constant heat flux condition is estimated to be distorted because of the conduction in the heating block and wall condition. The few previous experiments on saturated boiling found in the literature (Staniszewski, 1959; Han and Griffith, 1965; Cole and Shulman, 1966) did not show good repeatability for bubble growth, even in a series of data with the same experimental conditions. In this paper, we show that the local heating power should be controlled within a microsecond in order to maintain the same heating conditions during the inception of a bubble; this requirement may be related to the irregular behavior of the previous results. Recently, Rule et al. (1998) and Rule and Kim (1999) developed a microscale heater array that can be controlled at a high temporal and spatial resolution. A constant wall temperature can be achieved using the microscale heater array, and variation in the heat flow rate for a single bubble can be measured. In this study, the same heater array is used to maintain a constant wall temperature and to measure the heat flow rate. Since the heat flow rate to the bubble during growth is important for evaluating the heat transfer coefficient, precise measurement is of great interest.

2. Experiments

2.1. Experimental apparatus

The microscale heater array in detail described in Lee et al. (2003) was used to maintain heating surface as a constant wall temperature in this study. It was constructed on a transparent glass substrate using the VLSI technique. The Ti/Pt and Ti/Au layers were deposited using an electric beam evaporator to generate a heating surface and power leads. Each heater in the array had dimensions of 0.27×0.27 mm. A description of the device can be found in previous researches performed by Rule et al. (1998), Rule and Kim (1999) and Bae et al. (1999). Most of the experimental devices that have been used previously to control the power of the heating block beneath a bubble, and thereby provide a constant heat flux, could not maintain a constant surface

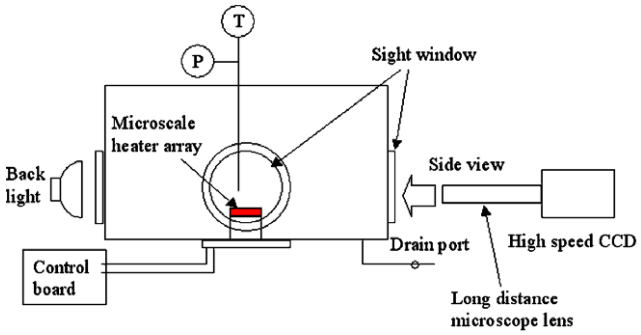

Fig. 1. Schematic diagram of the experimental apparatus.

temperature over very short time intervals. However, the present microscale heater array was controlled with a Wheatstone bridge circuit that could provide a constant surface temperature at a high temporal resolution. The longest time delay in the circuit occurred at the OP amp, which had a time resolution of 10^{-7} s. Due to the fast response of the circuit, good repeatability was achieved in the our experimental results. The voltage data for each heater can be sampled with 0.136 ms. And 1000 V readings for each heater can be memorized with the 12-bit resolution. The length of all tests performed in this study is 136 ms.

The temperature of 96 heaters in the array was controlled by 96 electric Wheatstone bridge feedback circuits, which be operated in a manner similar to constant-temperature hot-wire anemometry. Each heater in the array can be represented as one resistor in a Wheatstone bridge circuit. The calibration process for the wall temperature of heater was also described in Lee et al. (2003).

The data acquisition system was capable of sampling 16,000 data points from each heater at a speed of 7.35 kHz with 12-bit resolution. The data acquisition system was synchronized with a high-speed CCD camera system that recorded the images at a rate of 1000 or 4000 frames per second. A long-distance microscopic lens was also used to capture the bubble images during boiling (see Fig. 1).

Fig. 1 shows a schematic diagram of the boiling test chamber. The chamber was designed to provide three side views of bubble growth. Ten thin-film heaters to supply 15500 W/m^2 were attached to the sides of the chamber to control the pool temperature during the saturated pool boiling experiments. A 250-W halogen lamp mounted near the sight window on the opposite side of the high speed CCD camera was used as a backlight source. Backlighting allowed the camera to capture clearer images than lights mounted on the side of the chamber.

2.2. Uncertainty analysis

In the present study, the bubble growth behavior was analyzed using an equivalent radius of sphere with the same volume. The bubble volume was calculated using the measured bubble dimensions shown in Fig. 2, which were measured by counting the number of pixels in a captured image. A micrometer was placed in the chamber to provide guidance for the size measurements.

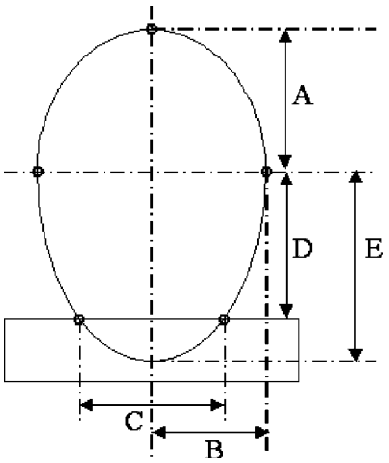

Fig. 2. Geometry of the spheroid used to determine the bubble volume.

Table 1
Experimental conditions

	Mass fraction of R11 [%]	$P_{sys.}$ [atm]	T_{sat} [°C]	T_{wall} [°C]	ΔT_{sup} [°C]	Ja [-]
R11	100	1	23.71	35.0	11.29	13.83
Mixture1	81.5	1	25.79	40.9	15.11	18.70
Mixture 2	53.6	1	29.91	43.1	13.19	19.55
Mixture 3	28.0	1	35.63	51.0	15.37	16.54
Mixture 4	13.9	1	40.43	54.9	14.47	18.66
R113	0	1	47.58	61.0	13.42	17.77
R11	100	1	23.71	37.1	13.39	16.40
				38.9	15.19	18.61

A physical dimension of 100 μm corresponded to 30 pixels for the cases that used pure R11 and Mixture 1 (see Table 1). One pixel in these images corresponded to 3.333 μm. For the other cases, 100 μm corresponded to 11 pixels, so one pixel in each image corresponded to 9.091 μm. The bubble dimensions were accurate within one pixel.

The equivalent bubble radius can be calculated using the measured bubble dimensions. Any measurement errors in the dimensions will propagate into the equivalent radius calculations. An uncertainty analysis for these calculations was performed using the method explained in Coleman and Steele (1989). The maximum uncertainty was 1.8% for the cases that used pure R11 and Mixture 1. For the other cases, the maximum uncertainty was 6.7% in the first image of pure R113. Excluding the first images, however, the uncertainties were less than 3.4%.

A thermocouple with 0.53 °C uncertainty was used to calibrate the temperature of the microscale heater array. The digital potentiometer in the Wheatstone bridge circuit had 512 digital positioning numbers. The Wheatstone bridge circuit was set to give a temperature displacement of 60 °C. Thus, one digit had a 0.12 °C temperature displacement and an uncertainty of 0.06 °C. The

maximum uncertainty of the calibrated temperature was 0.59 °C, which is the sum of the errors of the thermocouple and digital potentiometer: 0.53 and 0.06 °C, respectively.

The temperature difference between the bulk and the heating surface is measured to be 15 °C at maximum. The difference of refractive index of pure R113 is about 0.07% for the temperature difference of 15 °C. The distortion or refraction error caused at window as well as near heating surface liquid whose density differs from that of bulk liquid will be reasonably negligible. The data of refractive index of pure R113 was referred from page 18.3 in 1997 Fundamentals of ASHRAE Handbook and page 1640 in Handbook of Fine Chemicals and Laboratory Equipment of Aldrich (2001).

2.3. Experimental conditions

In the present study, saturated pool boiling experiments were conducted for six mixtures of R11 and R113 (see Table 1). The mass concentrations of R11 in the mixtures were chosen as like these cases including 100%, 81.5%, 53.6%, 28.0%, 13.9%, and 0%. We chose 100% and 0% cases as the reference, 53.6% as middle, 81.5% between maximum and middle, 28.0% and 13.9% (near mass concentration evaluated as minimum $|y-x|$ point of binary mixtures with R11 and R113) between minimum and middle.

Here, y is the mass fraction of the more volatile component, R11, on the vapor side, and x is the mass fraction of the more volatile component on the liquid side. The value of $|y-x|$ was evaluated from the bubble and dew lines of the R11 and R113 as binary mixtures.

3. Results and discussion

3.1. Experimental results for bubble growth of mixtures

Since most previous analytical analyses of bubble growth have considered a spherical bubble, the growth behavior in the present study was also analyzed using an equivalent radius. The equivalent radius (R_{eq}) is defined as the radius of a sphere with the same total volume (V_{total}) as the bubble measured in the experiments. If the bubble is axisymmetric and not vertically symmetric, then R_{eq} can be calculated as follows (Lee et al., 2003),

$$V_{total} = \frac{2}{3}\pi B^2 A + \frac{1}{3}\pi B^2 D\left[2 + \frac{(C/2)^2}{B^2}\right] = \frac{4}{3}\pi R_{eq}^3$$
$$R_{eq} = \left(\frac{1}{2}B^2 A + \frac{1}{4}B^2 D\left[2 + \frac{(C/2)^2}{B^2}\right]\right)^{1/3} \quad (4)$$

where A and B are the dimensions of the polar and equatorial radii respectively, in Fig. 2. C is contact diameter. D is the length between the cross point of polar and equatorial axis and heater surface. And E is calculated as Eq. (5).

$$E = \sqrt{\frac{D^2}{1 - \frac{(C/2)^2}{B^2}}} \tag{5}$$

The maximum uncertainty for equivalent bubble radius of the assumed half sphere of upper part and truncated ellipsoid of lower part (Fig. 2) was 3.8%.

Fig. 3 shows side view images of Mixture 2, which contains a 28% mass fraction of R11 (see Table 1). The bubble shapes shown in Fig. 3 are almost the same as those of pure R113 shown in Lee et al. (2003). The equivalent bubble radius during growth, shown in Fig. 4, indicates a slight difference between mixtures and pure fluids at the each near ONB temperatures. But the growth rate was also proportional to $t^{1/6} - t^{1/4}$ in the asymptotic growth region. The smallest power of time corresponded to the case of 28% R11, but the power of time did not depend on whether the bulk fluid was a mixture or pure. Hence we supposed that the power of time varied randomly;

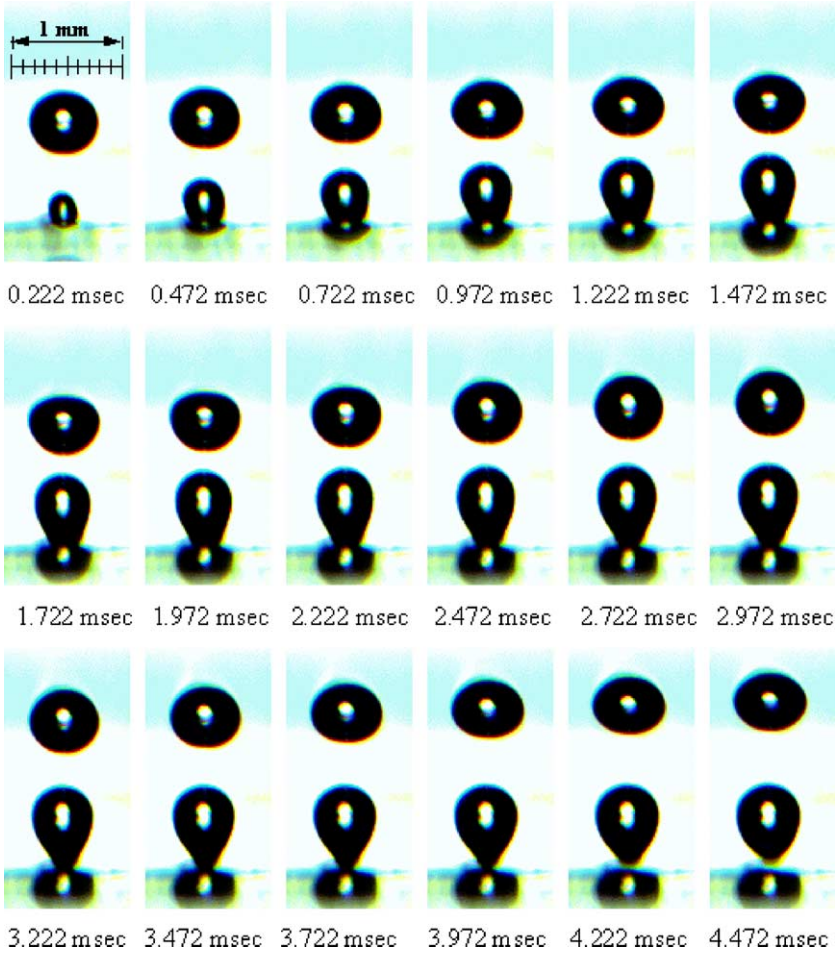

Fig. 3. Side view of a bubble for the case with 28% of R11 ($T_{wall} = 51.0$ °C).

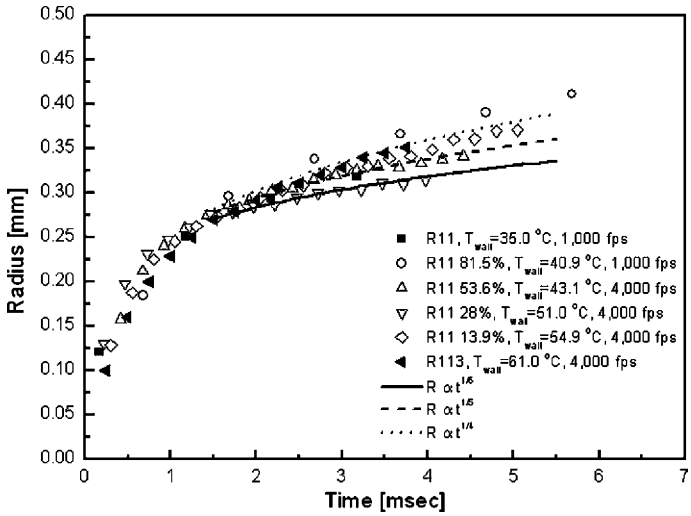

Fig. 4. Bubble growth behavior of mixtures for the each near ONB temperatures as pure fluids.

however, it was always less than one-third. Growth rates of less than time to the one-third power result in a decrease in the heat flow rate.

The appropriate dimensionless parameters reasonably chosen by Lee et al. (2003) were used to analyze the bubble growth at same scales. The dimensionless bubble radius, R^+, and time, t^+, can be expressed as

$$R^+ = \frac{R}{R_c}$$
$$t^+ = \frac{t}{t_c} \tag{6}$$

and the characteristic scales can be rewritten as

$$R_c = \sqrt{\frac{27}{2}} Ja\alpha \sqrt{\frac{\rho_l R_d}{2\sigma}}$$
$$t_c = \frac{9}{2} Ja\alpha \frac{\rho_l R_d}{2\sigma} \tag{7}$$

where ρ_l is the liquid density, σ is the surface tension of the liquid, and α is the thermal diffusivity of the liquid. Here, the Jakob number is defined by $(\rho_l C_{Pl} \Delta T_{sup})/(\rho_v h_{fg})$ and the wall superheat is $(\Delta T_{sup} = T_{wall} - T_{sat})$. This is because the bulk liquid is saturated, so the bubble growth should be influenced by the wall superheat. The departure radius (R_d) was also used as a scaling parameter to adjust the asymptotic growth behavior.

Fig. 5 shows the present results scaled using the dimensionless parameters of Eq. (7). There are good agreements between the results. And the bubble growth behavior for mixtures is very similar to that for pure fluids. Rayleigh (1917) showed that the growth rate under a constant pressure difference was proportional to t^+ which is reasonable during the initial growth. The latter part of

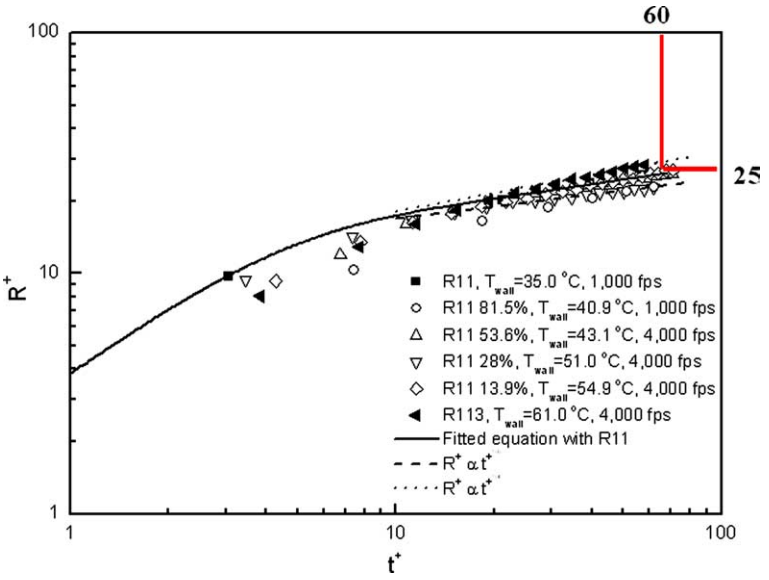

Fig. 5. Dimensionless behavior of bubble growth.

bubble growth is asymptotic and proportional to $t^{+1/5}$. Therefore, Lee et al. (2003) suggested a function of time t^+ that encompassed the global growth behavior as follows:

$$R^+(t^+) = 11.2t^{+1/5}\tanh\left(0.345t^{+4/5}\right) + 7.2\times 10^{-2} \tag{8}$$

This function, shown as a solid line in Fig. 5, agrees well with the present results.

The dimensionless departure time t_d and radius R_d were approximately 60 and 25, respectively, as shown in Fig. 5. Using the dimensionless parameters, suggested the following correlations:

$$R_d = \left[\frac{25}{2}\sqrt{27}Ja\alpha\sqrt{\frac{\rho_l}{\sigma}}\right]^2 \tag{9}$$

$$t_d = 135Ja\alpha\frac{\rho_l R_d}{\sigma} \tag{10}$$

A comparison between the present results and some previous experimental results using these correlations is shown in Fig. 6. The departure radius and time could be well predicted within a 30% error.

The bubble growth rate for binary mixtures is compared to that of pure fluids under almost the same wall superheat conditions in Fig. 7. The wall superheat for the mixtures at the ONB was approximately 15, and the wall superheat of R11 for a wall temperature of 38.9 °C was also approximately 15, as shown in Table 1. The bubble radius and time of the mixtures were smaller than these of R11. This is directly related with the reduction of the heat flow rate and the heat transfer coefficient. This phenomenon agrees well with results reported by previous researchers (Stephan and Korner, 1969; Calus and Leonidopoulos, 1974; Unal, 1986).

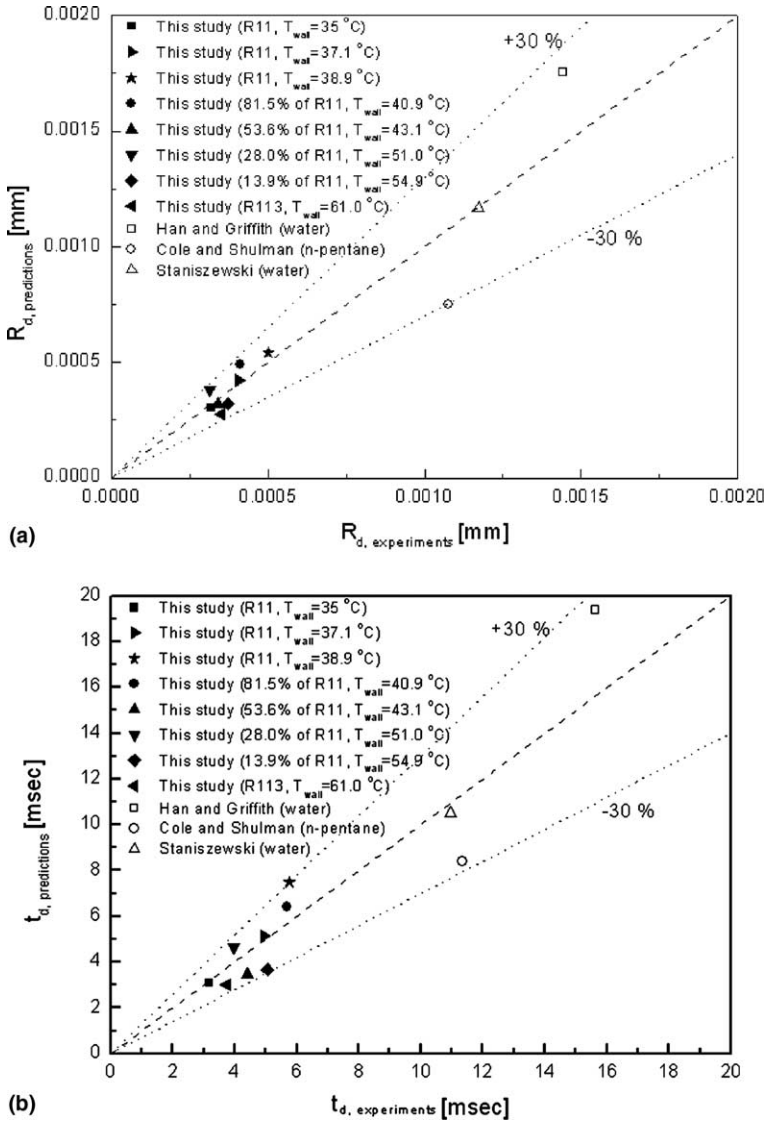

Fig. 6. Comparison of the departure radius and time: (a) departure radius and (b) departure time.

3.2. Reduction of the heat transfer coefficient of binary mixtures

In previous researches, the reduction of the heat transfer coefficient in boiling of binary mixture was reported that happened the greatest at low mass concentrations of the more volatile component. Therefore, two cases with lower mass concentrations were chosen to confirm the reported reduction of the heat transfer coefficient.

In the present experiments, the wall superheat at the ONB for binary mixtures was usually larger than that for pure fluids, as shown in Table 1. We examined the effect of wall superheat increase on the heat transfer coefficients, which are shown in Fig. 8(a). The filled circle symbols

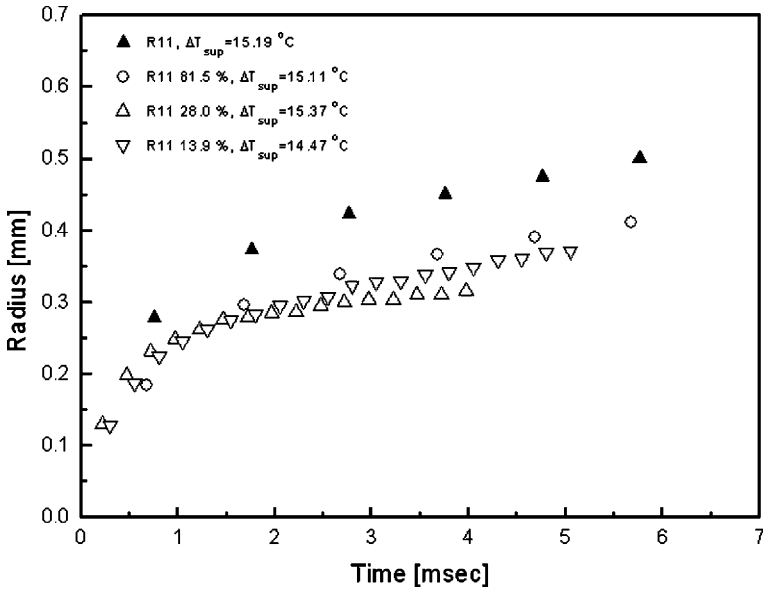

Fig. 7. Comparison of bubble growth in mixtures and pure fluids with almost the same wall superheat.

represent the experimental results, and the blank symbols represent the predictions of the previous studies. The heat transfer coefficient for the present experiments was evaluated using the average required heat flux for bubble growth and the wall superheat ΔT_{sup}

$$h = \frac{q''_{\text{average}}}{\Delta T_{\text{sup}}} \tag{11}$$

The present experiments were conducted with a constant wall temperature condition, not a constant heat flux condition. For constant wall temperatures, the heat flow rate data showed a discernible peak in the initial growth region as reported in Lee et al. (2003). Thus, the average heat flux for the heat transfer coefficient was evaluated using the time averaged heat flow rate required for bubble growth

$$q''_{\text{average}} = \frac{\int_{t=0}^{t=t_{\text{d}}} \dot{q}\,\mathrm{d}t}{At_{\text{d}}} \tag{12}$$

where $\dot{q}$ is the required heat flow rate for bubble growth, t_{d} is the departure time, and A is the bubble surface area of the microscale heater where the bubble is attached.

The minimum heat transfer coefficients in Fig. 8(a) occurred near the maximum $|y-x|$ values in Fig. 8(b) as reported in the previous researches. This heat transfer coefficient behavior agrees somewhat with that reported in previous studies.

All previous correlations like as Eqs. (1)–(3) contain the resistance factor, $|y-x|$. This reduction factor appears in the theoretical analyses of Scriven (1959) and Van Stralen (1966), who derived the growth equation for a mixture from the growth equation of a pure fluid using the mass diffusion at the interface. Based on their analyses, previous researchers have suggested many correlations for the heat transfer coefficient of binary mixtures using the reduction factor, $|y-x|$.

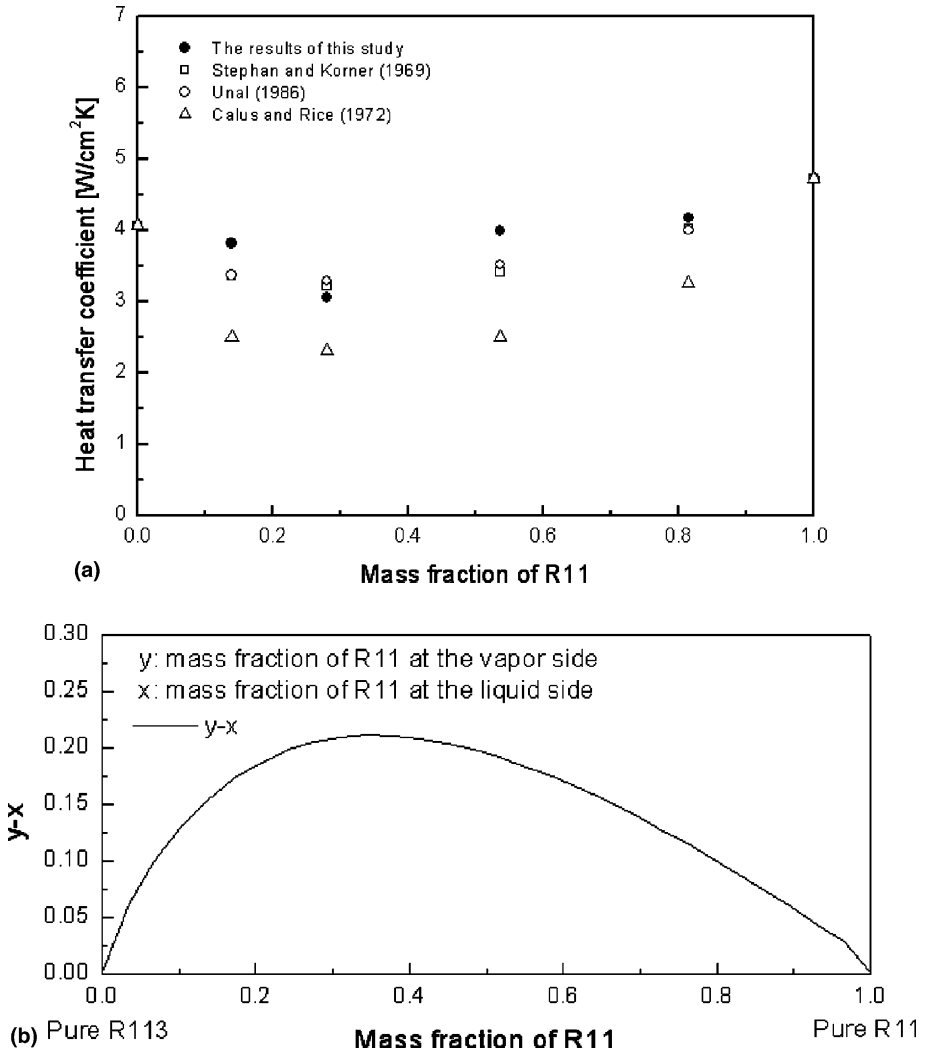

Fig. 8. Heat transfer coefficient of mixtures: (a) heat transfer coefficient; (b) variation of y–x as a function of the R11 mass fraction.

However, these correlations assumed a constant bubble frequency, bubble growth, nucleation site density, and ONB temperature. All of these factors can affect the heat flow rate and the heat transfer coefficient characteristics.

In the present experiments, the heat transfer coefficient was evaluated for single bubble growth over one period at one nucleation site with a constant wall temperature. The wall superheat (i.e., the denominator in the heat transfer coefficient calculation equation) increased for binary mixtures, as shown in Table 1. Even though the wall superheat of binary mixtures was higher for the same ONB conditions (ΔT_{ONB}), the bubble radius in binary mixtures was only slightly larger than that in pure fluids, as shown in Fig. 4, and there was little difference between the average heat fluxes. This is despite the fact that the bubble radius was directly related to the heat flow rate. The

increased ΔT_{ONB} led to a reduction in the heat transfer coefficients of binary mixtures. For the same ONB conditions, the effect of the increased ΔT_{ONB} on the reduction in the heat transfer coefficient of binary mixtures was comparable to the effect of the reduction in bubble growth.

4. Conclusions

Nucleate pool boiling experiments for binary mixtures, which consisted of R11 and R113, were performed with constant wall temperature condition. The wall temperature could be precisely controlled using a microscale heater array and Wheatstone bridge circuits, and the local and instantaneous heat flow rates were measured at high temporal resolutions. Time-triggered high-speed CCD images were captured at sampling rates of 1000 and 4000 Hz and synchronized with heat flow rate measurements to analyze the bubble motion.

The geometry of the bubble was obtained from the captured bubble images. The equivalent radius of a sphere of the same volume showed a small shape assumption error. There was no discernible difference in the bubble growth behavior of binary mixtures and pure fluids. In the asymptotic growth region, the bubble growth rate was proportional to a value between $t^{1/6}$ and $t^{1/4}$ which was slower than the growth rate reported in previous analytical analyses. The dimensional departure radius and time for mixtures was smaller than these of pure fluids under the almost same ONB conditions, and the mixtures usually showed a greater ONB temperature difference (ΔT_{ONB}) than pure fluids.

Bubble growth behavior was analyzed using dimensionless parameters to compare mixtures with pure fluids as the same scales. The comparisons showed good agreement in the asymptotic growth region. The dimensionless departure time and radius were approximately 60 and 25, respectively.

The minimum heat transfer coefficient of mixtures occurred near the maximum $|y - x|$ value, which agrees with previous studies. Under the almost same ONB conditions, the average heat flux did not depend on the mass fraction of R11, and the effect of the greater ΔT_{ONB} for mixtures on the heat transfer coefficient deterioration was comparable to the effect of the reduction in bubble growth.

Acknowledgements

This work was supported by the Ministry of Science and Technology of Korea through the National Research Laboratory program. The authors are grateful to Prof. Jungho Kim for providing the basic design of the microscale heater array including its controller, Dr. Sung Won Bae for providing the basic data for binary mixtures, and to the Samsung Advanced Institute of Technology for fabricating the microscale heater array.

References

Bae, S.W., Kim, J., Kim, M.H., 1999. Improved technique to measure time- and space-resolved heat transfer under single bubbles during saturated pool boiling of FC-72. Exper. Heat Transfer 12, 265–279.

Calus, W.F., Leonidopoulos, D.J., 1974. Pool boiling—binary liquid mixtures. Int. J. Heat Mass Transfer 17, 249–256.
Calus, W.F., Rice, P., 1972. Pool boiling—binary mixtures. Chem. Eng. Sci. 27, 1687–1697.
Celata, G.P., Cumo, M., Setaro, T., 1994. A review of pool and forced convective boiling of binary mixtures. Exper. Therm. Fluid Sci. 9, 367–381.
Cole, R., Shulman, H.L., 1966. Bubble growth rates at high Jakob numbers. Int. J. Heat Mass Transfer 9, 1377–1390.
Coleman, H.W., Steele Jr., W.G., 1989. Experimentation and Uncertainty Analysis for Engineers. John Wiley & Sons Inc., New York, USA.
Han, C.H., Griffith, P., 1965. The mechanism of heat transfer in nucleate pool boiling—part I bubble initiation, growth and departure. Int. J. Heat Mass Transfer 8, 887–904.
Lee, H.C., Oh, B.D., Bae, S.W., Kim, M.H., 2003. Single bubble growth in saturated pool boiling on a constant wall temperature surface. Int. J. Multiphase Flow. 29, 1857–1874.
Rayleigh, J.W.S., 1917. On the pressure developed in a liquid during the collapse of a spherical cavity. Philos. Mag. 34, 94–98.
Rule, T.D., Kim, J., Kalkur, T.S., 1998. Design, construction and qualification of a microscale heater array for use in boiling heat transfer. NASA/CR-1998-207407.
Rule, T.D., Kim, J., 1999. Heat transfer behavior on small horizontal heaters during pool boiling. J. Heat Transfer 121, 386–393.
Scriven, L.E., 1959. On the dynamics of phase growth. Chem. Eng. Sci. 10, 1–13.
Staniszewski, B.E., 1959. Nucleate boiling bubble growth and departure. MIT DSR Project No. 7-7673, Technical Report No. 16.
Stephan, K., Korner, M., 1969. Berechnung des Warmeubergangs verdampfender binarer Flussigkeitsgemische. Chem. Ing. Tech. 41, 409–417.
Unal, H.C., 1986. Prediction of nucleate pool boiling heat transfer coefficients for binary mixtures. Int. J. Heat Mass Transfer 29, 637–640.
Van Stralen, S.J.D., 1966. The mechanism of nucleate boiling in pure liquids and in binary mixtures—Part II. Int. J. Heat Mass Transfer 9, 1021–1046.